Influence of the wood mechanical properties in the dovetail joint behavior

K. Šobra & P. Fajman
Department of Mechanics, Faculty of Civil Engineering, Czech Technical University in Prague, Czech Republic

J. M. Branco
ISISE, Department of Civil Engineering, School of Engineering, University of Minho, Guimarães, Portugal

ABSTRACT: The force distribution inside a dovetail joint is complex. Wood is simultaneously loaded in different directions in the several connected surfaces. The analytical solutions available for the analysis of the behavior of those carpentry joints rely on the mechanical properties of wood. In particular, the stiffness properties of wood under compression are crucial for the forces equilibrium. Simulations showed that the stiffness values considered in each of the springs normally assumed in the analytical models, have great influence in the bearing capacity and stiffness of the dovetail joints, with important consequence on the stress distribution over the overall structure. In a wide experimental campaign, the properties under compression of the most common wood species of existing timber structures have been determined. Then, a solved example of a dovetail joint is presented assuming different wood species and the corresponding strength and stiffness properties values obtained in the tests.

1 INTRODUCTION

Wood is an organic material, which in comparison with other mainly inorganic building materials, has height variability of its properties. Moreover, wood is orthotropic and heterogeneous material, thus its mechanical properties are depended not only at the direction and position (occurrence of knots), but also, for example, on the moisture content.

Variability of mechanical properties of wood complicates the design of timber structural elements. Traditional carpentry joints can be mentioned as an example. Utilization of carpentry joints grows with renewed popularity of timber structures. Furthermore, utilization of traditional carpentry joints is demanded at reparation of historical structures and monuments, when is due to Historical preservation paid attention to a preservation of the originality of a construction and a material. The design of traditional carpentry joints in not in the Czech Republic supported by any guidelines and it is mainly depended on the carpenter experience and skills. Despite traditional carpentry joints are constructed still in the same way during the ages, there are not sufficient amount of studies, nowadays, such as (Branco et al., 2006a; Branco et al., 2006b; Jasienko et al., 2006; Parisi & Cordié, 2010; Parisi & Piazza, 2000; Sangree & Schafer, 2009a; Sangree & Schafer, 2009b; Villar et al., 2007), which can help examine their behaviour. Thus, there is a vast research project running currently in the Czech Republic supported by the Czech Ministry of Culture, which is focused on traditional carpentry joints (Arciszewska-Kędzior et al., 2015; Fajman, 2014; Fajman & Máca, 2014; Kunecký et al., 2015).

Issues related with variability of material properties of wood and with the structure of the wood as a whole were shown many times during the project. Defects, unseen by human eye, spoiled evaluation of experiments as well as a work on determination of typical failure mechanisms of specific construction during particular loading. The joint behaviour influenced by the

mechanical properties variability can be shown on the example of traditional carpentry joint, a dovetail joint.

2 EXPERIMENTAL CAMPAIGN

For the formulation of the dovetail joint analytical solution, which is briefly described at (Šobra et al., 2015), the compressive normal stiffness developed in the contacted surfaces is needed. Since values of compressive stiffness are depended on dimension of element, it cannot be easily found at literature. Therefore, it was decided to make an experimental campaign aimed to establish this property for the most common wood species that can be found on existing timber structures. Experiments, which results are further presented, were performed at the University of Minho, Portugal.

Since the experiments were made in cooperation of Portuguese University of Minho and the Czech Technical University in Prague, only the most widely spread wood species for both countries were examined. Therefore, specimens made of four wood species were prepared, namely the Scots Pine (*Pinus sylvestris*, specimens created form this wood species are labelled as "SP"), the Silver Fir (*Abies alba*, "SF"), the Chestnut (*Castanea sativa*, "Ch") and the Maritime Pine (*Pinus pinaster*, "MP") were used. First two wood species are typical for the Czech Republic, whereas remaining two species are typical for Portugal. Since only values of mechanical properties in compression were required for creation of the analytical solution, only compression test were made. Therefore, specimens made according to European standard EN 408 (CEN, 2010) were prepared. Those specimens are further labelled as "C".

Verification of the influence of a load spreading, which influences stresses under the loading, should be also one of the outputs of the campaign. Despite this approach have been described by Leijten and van der Put in (Leijten et al., 2012; Leijten et al., 2010; Put, 2008) just for the compression perpendicular to the grain, it is used in the Eurocode 5 - EN 1995-1-1 (CEN, 2006) (further called EC 5). Thanks to the geometry of a dovetail joint (seen at Fig. 6), the joint is compressed in various angle to the grain, thus, an effort to evaluate the loading spreading angled to the grain was made. For purposes of the evaluation of the load spreading specimens made according to US standard ASTM D143-14 (ASTM, 2014) were also prepared for the campaign. Those specimens, further marked as "VP", have different dimensions than "C" specimens and allow the spreading of the loading. Comparison of the dimensions of prepared specimens is shown at Figure 1.

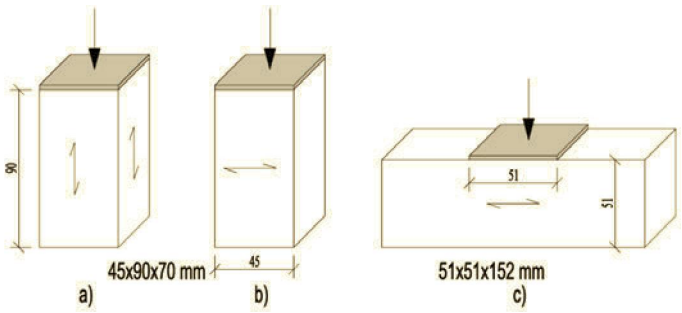

Figure 1. Specimens dimensions; a) and b) according to EN 408 (CEN, 2010) and c) according to ASTM D143-14 (ASTM, 2014).

Further, an effort to discover if Hankinson's expression (1) can be also used for other material characteristics was done. The Hankinson's formula can be used for recalculation of the wood compressive strength angled to the grain just from the compressive strength parallel and perpendicular to the grain, Therefore, "C" and "VP" specimens were prepared for possibility of evaluation of mechanical properties parallel to the grain (further labelled "0"), perpendicular to the grain ("90") and angled in an angle 45° to the grain ("45"). Six specimens from each combi-

nation of dimensions, species and the grain angle were tested, what means 120 specimens were tested overall. Only exception makes "VP" specimens in the compression parallel to the grain, which were not tested.

$$f_{c,\beta,d} = \frac{f_{c,0,d}}{\frac{f_{c,0,d}}{f_{c,90,d}} \sin^2 \beta + \cos^2 \beta} \tag{1}$$

where $f_{c,\beta,d}$ is the compressive strength under the angle β to the grain, $f_{c,0,d}$ is the compressive strength parallel to the grain and $f_{c,90,d}$ is the compressive strength perpendicular to the grain.

Experiments setup for the specimens made according to EN 408 (CEN, 2010), is noticeable at Fiure. 2a) and fastening of LVDTs on the side surfaces of the specimens is shown at Fiure. 2b). Since one LVDT was places directly on the force actuator, comparison of values obtained from both types of LVDTs is possible. At the basis of this comparison, measured displacements and results evaluated from them were separated into two groups. In comparison with side LVDTs, the LVDT placed at the force actuator shown higher values of deformation, what points to higher local deformation of the specimen under the spread plate, thus, result evaluated from this LVDT are marked as "local". Since side LVDTs were not influenced by local higher deformation of specimens under spread plate, it is assumed, that deformation measured by them corresponds with the behaviour of the specimens as a whole, and thus, values evaluated from them are further labelled as "global".

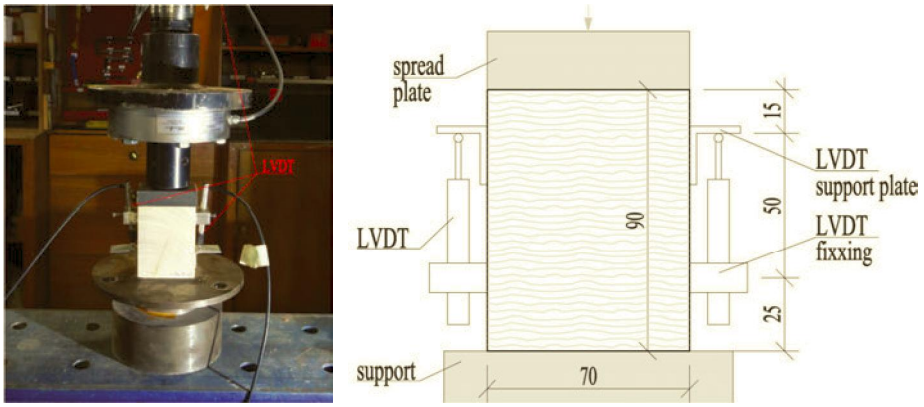

a) b)

Fiure. 2. a) the experimental arrangement, b) measured length on the specimen prepared according to EN 408 (CEN, 2010).

Data measured during experiments were evaluated according to approaches mentioned in European standard EN 408 (CEN, 2010), where is the modulus of elasticity calculated according to expression (2) and the compressive strength is evaluated according to expression (3).

$$E_{c,90} = \frac{(F_{40} - F_{10}) h_0}{(w_{40} - w_{10}) bl} \tag{2}$$

$$f_{c,90} = \frac{F_{c,90,\max}}{bl} \tag{3}$$

where $E_{c,90}$ is the modulus of elasticity perpendicular to the grain, F_{40} and F_{10} is 0.4 respectively 0.1 of the maximal force $F_{c,max}$, w_{40} and w_{10} is the displacement corresponding with force F_{40}, respectively with F_{10}, h_0 is the measured length, b is the width and l is the length of the specimen and $f_{c,90}$ is the compressive strength perpendicular to the grain.

At Figure 3a) is shown EN approach for determination of values used in equations (2) and (3). Since US standard (ASTM, 2014) uses different dimensions of specimens, the approach for data processing is different too. Comparison of both the EN and the US approaches is shown at Figure 3.

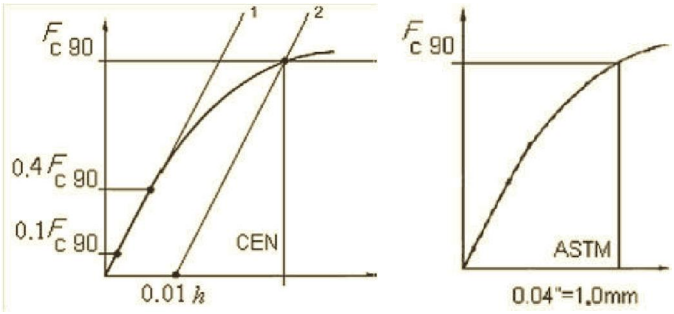

a) b)

Figure 3. Ways of finding $F_{c,max}$ according to EN 408 (CEN, 2010) a) and according to ASTM (ASTM, 2014) b).

The stiffness of tested specimens, which was one of the main reasons for realization of experimental campaign, was evaluated from force-displacement relationship with utilization of principle of balance of potential energy. Since the proportional limit was not usually easy to determine from the force-displacement relationship, obtained curves were substituted with bi-linear behaviour (see Fig. 4). Assumption of potential energies equilibrium is applied as follows. Square area below the force-displacement curve representing the potential energy has to be equal to square area below the bi-linear simplification. Using this approach virtual proportional limit used for the stiffness evaluation is clearly defined (red square at Fig. 4). Using the energy balance, the elastic stiffness (K_e, based on the red full line at Fig. 4) can be easily determined as well as estimated evaluation of post-elastic stiffness (K_p, based on the red dashed line at Fig. 4) can be made.

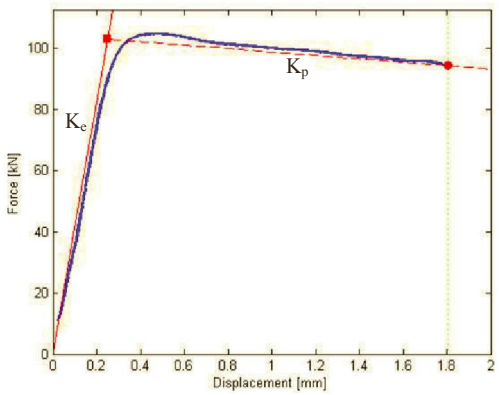

Figure 4. Example of application of bilinear approximation.

Evaluated stiffness's of Silver Fir with grain angle of 45° are shown at Table 1. In the table are shown both global and local stiffness's for each specimen in a series. Since height of ASTM specimens is short, measurements of global deformation is not possible there, therefore, global stiffness of "VP" specimens was not evaluated. Big differences in K_e and $K_{e,ASTM}$ values, which are in both cases elastic stiffness's, is surprising, although similar values of the stiffness for both types of specimens were expected, because both specimens have similar loaded square area. The difference between stiffness's can be explained by differences in approaches for evaluation of the force, which can be used for the stiffness evaluation, how it is shown in Figure 4. The force in case of ASTM approach is firmly established for the displacement of 1mm, whereas the EN approach works with force close to the proportional limit. On the account of this can be noted, that way of evaluation influences evaluated values.

Table 1. Evaluated stiffness's for Silver Fir, $\cdot 10^3$ [kN/m].

Local	SF-C-45		SF-VP-45			Global	SF-C-45	
	K_e	K_p	K_{e_ASTM}	K_e	K_p		K_e	K_p
"1"	14.667	0.575	8.83	22.963	1.164		77.241	1.153
"2"	10.87	-0.042	9.33	22.963	2.291		52.222	0.770
"3"	13.077	0.895	11.36	19.286	1.369		109.375	18.56
"4"	14.167	0.742	10.56	21.481	1.044		109.375	17.09
"5"	12.333	0.736	9.79	21.739	1.388		111.765	20.06
"6"	13.176	0.272	9.295	20	2.464		48.222	1036
Average	13.05	0.53	9.86	21.41	1.62		84.7	14.22
CoV.	0.103	0.536	0.098	0.07	0.438		0.318	0.351

At Table 1 labelling *Local* and *Global* explains what kind of stiffness's is shown at the part of the table on the right from the label, K_e means the elastic stiffness, K_p means the post elastic stiffness and K_{e_ASTM} means the elastic stiffness evaluated according to the ASTM approach, *Average* is the average value and *CoV.* is the coefficient of variation of the shown values.

During the evaluation of experiments, values of the compressive strengths and densities of each wood species were also obtained. Those results are presented at Table 2.

Table 2. Obtained average strengths and density.

	C-90 [MPa]	VP-90 [MPa]	C-45 [MPa]	VP-45 [MPa]	C-0 [MPa]	Density [kg/m^3]
Silver fir (SF)	3.29	5.43	6.76	11.1	32.36	422.61
Chestnut (Ch)	6.6	16.98	14.43	22.15	47.42	647.75
Scots pine (SP)	4.08	7.25	6.07	12.03	48.9	545.36
Maritime pine (MP)	6.99	15.51	18.14	24.9	40.53	624.58

It can be noticed, that evaluated results are much higher than expected ones. On the bases of visual survey all softwood specimens were classified as C24, what means, that characteristic compressive strengths according to EN 338 (CEN, 2003) is 24MPa for the compression parallel to the grain and 2.5MPa for the compression perpendicular to the grain.

Comparison of obtained values of the compressive strength for "C" specimens normalized to maximal value of the strength to 1 with theoretical values using Hankinson's formula used in EC 5 (CEN, 2006) is shown at Figure 5.

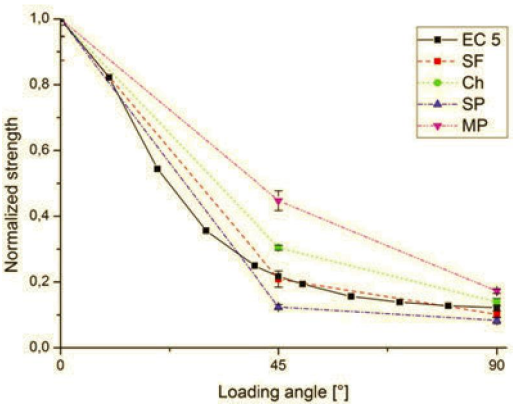

Figure 5. Obtained strengths with the standard deviation influenced by loading angle in comparison with the behaviour assumed by EC 5 (CEN, 2006).

3 DOVETAIL JOINT

Values evaluated from experiments were used to create an analytical solution for dovetail joints. As was written in introduction, a dovetail joint is one of typical (historical) carpentry joints, which can be found mainly in collar beam trusses and in construction of high roofs, which are one of the main architectonical signs of Gothic period. The joint can connect two elements in various angles. The position of connecting elements is secured by a wooden key, usually made form hardwood. One of the main advantages of the joint is its capability to transfer any combination of loading, both normal forces and rotations. Example of one-sided dovetail joint is shown at Figure 6a) and its utilization in various places in a truss is shown at Figure 6b).

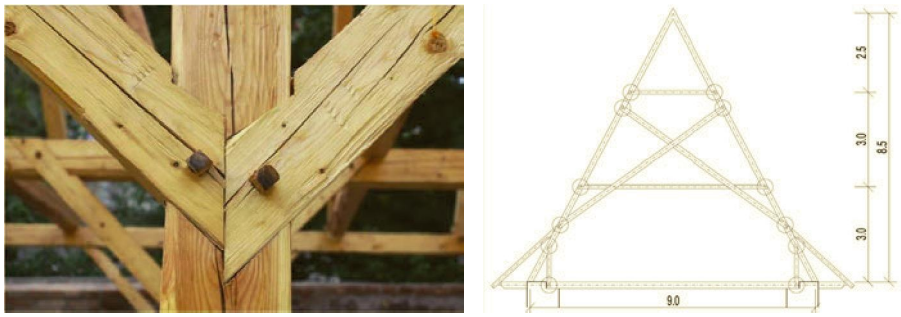

a) * b)

Figure 6. a) Connection of struts with a post using two one-sided dovetail joints and b) utilization of dovetail joints in a collar beam truss of Church of Saint Anna in Prague (Czech Republic) – dovetail joints are in circles. * www.tesarskahut.cz_galerie_img-04911374995661.

3.1 *Analytical solution*

Forces in a dovetail joint are transferred through direct contact with support of the friction on common contact areas for both elements. An analytical solution which uses this assumption for a calculation of forces distribution within the joint and which is described in (Šobra, et al., 2015) is further briefly introduced. Contact forces according to Figure 7 (for cases of compression and clockwise rotation of the joint) are placed into centres of mass of each contact (compressive) area in the analytical solution. Thanks to various effects, the stress of compressive area can be unequal, thus points of action of forces can be shifted. This effect was considered

and described with additional unknown bending moment placed into the centre of mass of corresponding contact area. Thus, meaning of the additional bending moment is possible eccentricity of contact forces. Since the resultants of forces act as statically indeterminate construction, they are calculated using the force method, which is based on the Castigliano's variational principle (4), which solves minimum of complementary energy of a system.

$$\Pi^* = \int_{\Omega} {}^*(\boldsymbol{\sigma}) \; \Omega - \int_{\Gamma} \boldsymbol{\sigma}^T \boldsymbol{n}^T \bar{\boldsymbol{u}} \; \Gamma = min. \tag{4}$$

where Π^* is the complementary energy of a system, W^* is the complementary energy of internal forces, Ω is the volume of a body and Γ is its border, $\boldsymbol{\sigma}$ is the tensor field of stresses, $\bar{\boldsymbol{u}}$ is the tensor field of strains and $\boldsymbol{n}$ is the matrix of directional cosines.

Three forces are chosen at the beginning of the solution. Those forces have to fulfil static and geometrical equations to create statically defined supports of a construction. Remaining forces which act in the joint are replaced by statically indeterminate forces, which in further calculation loading the joint step by step. Specific course of internal forces, which belongs to each loading state, is used to further calculation of coefficients of flexibility δ_{ij}. Coefficients of flexibility are calculated using integration of mentioned course of internal forces related to the axis of the skew element (5). General theoretically assumed internal forces courses are shown on the right of the joint at Figure 7a). Since geometry of a dovetail joint is complicated, the beginning and the end of solved intervals assumed during integration of internal forces course can have different values of cross-section and material characteristics. Since those values are usually considered as constant during integration, it is necessary to calculate those integrals numerically dividing intervals into subintervals. Constant or linear change of the stiffness on each subinterval can be assumed.

After establishment of the coefficients of flexibility, values of statically indeterminate forces are calculated from a set of linear equations (6). Remaining forces (supports chosen at the beginning of method) are calculated either from conditions of equilibrium or using of principle of superposition. The resultants of forces during compression by force 10kN are shown at Table 3. For the calculation was used the same arrangement of the joint which corresponds with scaled models in a ration 1:2 which were tested at the University of Minho. Specifically, two elements, horizontal "el. 1" with dimensions: the width of the element B = 60mm and the height of the element H = 100mm and the skew element "el. 2" with the width of the cross-section of b = 60mm and with the height h = 80mm were connected under the angle α = 60°, the joint was held together by a dowel with the diameter d = 20mm. Both elements were made from Scots Pine (*Pinus sylvestris*) which had experimentally evaluated mechanical properties: the modulus of elasticity parallel to the grain E_0 = 43930 MPa, the modulus of elasticity perpendicular to the grain E_{90} = 1402MPa, the compressive strength parallel to the grain $f_{c,0}$ = 48.9MPa and the compressive strength perpendicular to the grain $f_{c,90}$ = 4.08MPa.

$$\delta_{ij} = \int \frac{M \cdot \bar{M}}{EI} + \int \frac{N \cdot \bar{N}}{EA} + \int \frac{V \cdot \bar{V}}{GA} ds \tag{5}$$

$$\begin{aligned} &\delta_{11} \cdot {}_1 + \delta_{12} \cdot {}_2 + \mathrm{K} + \delta_{1n} \cdot {}_n + \delta_{10} = 0 \\ &\mathrm{M} \\ &\delta_{n1} \cdot {}_1 + \delta_{n2} \cdot {}_2 + \mathrm{K} + \delta_{nn} \cdot {}_n + \delta_{n0} = 0 \end{aligned} \tag{6}$$

$$G = \frac{E}{2(1-\nu)} \tag{7}$$

where δ_{ij} are coefficients of flexibility, X_i are statically indeterminate forces, M symbolizes bending moment course, N is a course of the normal force and V is a course of the shear force, E is the modulus of elasticity, I is the moment of inertia of a cross-section, A is the square area and G is the shear modulus calculated according to equation (7), where ν is the Poisson's ratio.

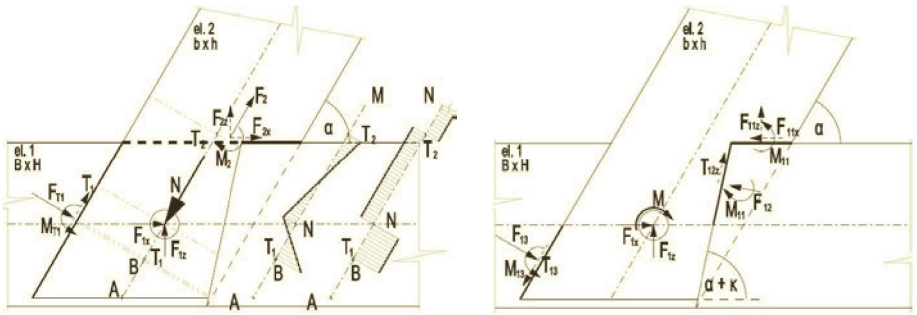

a) b)

Figure 7. Considered forces according to principle of virtual work a) during compression with general bending moment "M" and normal force "N" diagrams and b) during clockwise bending moment.

At this place is necessary to make notes about models used for the calculation of a dovetail joint by force method. An effect of friction can be assumed at the left compressive area of the skew element. Nevertheless, the friction is conditioned by existence of the force perpendicular to the estimated surface. If resultant of this force is tension, it is not possible to calculate with the friction and a simplified model, which does not considers the friction and forces on the corresponding compressive area is used. In the case, when the perpendicular force is compressive, calculated friction force can by higher than value $\mu \cdot F_T$, where μ is the coefficient of friction. In this case is used model, which prescribes the friction force as $\mu \cdot F_T$. This value is then supplemented to the value of the perpendicular force, which newly has value $F_T + \mu \cdot F_T$. Described conditions can be used for each surface, where the friction is considered.

On the basis of above mentioned assumptions, the following models were established:

- $T + F_{2x+y}$, this model considers the friction at the left surface of the skew plate. Nevertheless, the perpendicular force includes friction with its value $\mu \cdot F_{T1}$, that means that the final perpendicular force is $F_{T1} + \mu \cdot F_{T1}$. Force F_2, which is parallel with the axes of the skew element, is divided into its orthogonal parts - perpendicular to the compressive area (F_{2z}) and F_{2x} which represents the friction force and it is parallel with the surface of the compressive area. In this model, seven unknown forces are considered.
- $T + F_2$, the friction on the left surface of the skew plate is considered again in this model and it is considered in the same way as was described in the $T + F_{2x+y}$ case. A difference against the previous model is in the force F_2. The friction force F_{2x} and the perpendicular force F_{2z} are put together to the force F_2, which is parallel to the grain and during the calculation has form $F_2 + \mu \cdot F_2$. Since the friction force F_{2x} is considered in the force F_2, this model has six unknown forces.
- F_{2x+y}, this model assumes that the force F_{T1}, perpendicular to the left surface of the skew element, is tensile. Since no friction arises and thanks to geometric imperfections, there is a gap between the two elements of the joint, thus, the tensile force cannot be transfer through the direct contact to the horizontal element. The force at the left compressive area of the skew element is not considered in this model. The same assumption described in the model $T + F_{2x+y}$ is used for the force F_2. Since the forces at the left compressive area of the skew plate were neglected, the model calculates with five unknown forces.
- F_2, forces on the left compressive area of the skew plate are neglected and the friction force on the upper surface of the horizontal element is considered in the force F_2, like described at the model $T + F_2$. Thus, the model works only with four unknown forces.

Values of forces, which in Table 3 have grey background, symbolize non-fulfilment of any above mentioned condition. Therefore, those kinds of result are not sufficiently representative for given type of loading and used model of calculation. If assumed forces are in the model parallel with the axis of the skew element, they are for better comparison recalculated to the orthogonal coordinates corresponding with global system of coordinates.

Table 3. Force distribution within the joint during compression, loading force N = 10kN (projection to x direction: -5kN; y projection: -8.66kN), influence of normal and shear fore is considered, friction $\mu = 0$.

Type of solution	Considered forces [kN]							
	$F_{key\,x}$	$F_{key\,z}$	$F_{T1\,x}$	$F_{T1\,z}$	M_{T1}	F_{2x}	F_{2z}	M_2
$T + F_{2x+y}$ (7 forces)	0.0472	0.0174	-0.131	0.076	0.231	5.084	8.567	0.068
$T + F_2$ (6 forces)	5.245	6.429	-0.245	0.142	-0.0115	0	2.09	0.058
F_{2x+y} (5 forces)	10	17.321	-	-	-	-5	-8.66	-0.067
F_2 (4 forces)	5	-2.886	-	-	-	0	11.546	0.422

4 CONCLUSION

From above mentioned is noticeable that forces resultants are depended mainly on the modulus of elasticity, more precisely, on the ration between modulus's of elasticity for each internal forces (normal forces, shear and bending moment). If the influence of the normal force and the bending moment is investigated, it is necessary to change ratios between particular coefficients of flexibility, that means change the value of the modulus of elasticity separately for the influence of normal force and for the influence of the bending moment. The shear force also influences final solution; however, as was mentioned above, shear modulus is calculated from modulus of elasticity already used for normal force or bending moment. Since the shear force is dependent quantity, its behaviour is in comparison presented bellow wilfully neglected - the shear coefficient of flexibility are always depended on one of the couple - normal force and bending moment.

When increasing the normal stiffness, values of forces in the joint change its values significantly, how is possible to see from Table 4. In case of compression, forces eccentric to the axis of skew element decrease their values with increasing normal stiffness and whole loading is transferred just by the dowel. Nevertheless, significant change of forces magnitudes occurs when the normal stiffness is many times higher than the bending stiffness, more precisely, when the normal compliance is neglected.

Table 4. Force distribution within the joint during compression, loading force N = 10kN (projection to x direction: -5kN; y projection: -8.66kN), influence of normal force is considered, friction $\mu = 0.4$.

Type of solution	N/M	Considered forces [kN]							
		$F_{T1\,x}$	$F_{T1\,z}$	M_{T1}	$F_{key\,x}$	$F_{key\,z}$	F_{2x}	F_{2z}	M_2
$T + F_{2x+y}$ (7 forces)	1	-0.008	0.057	0.347	0.362	-0.051	4.58	8.72	0.215
	1000	0.003	-0.001	-0.007	4.724	0.518	0.272	0.518	-0.013
	∞	7.727 e-09	-1.113 e-09	-0.029	5	8.66	5.189 e-09	8.222 e-09	-2.14 e-10
$T + F_2$ (6 forces)	1	-0.33	0.048	-0.03	4.86	6.593	0.466	2.02	-0.019
	1000	-0.001	0.001	0.001	5	8.66	0.001	0.003	-0.001
	∞	-1.822 e-12	2.626 e-13	-2.678 e-13	5	8.66	5.733 e-12	2.482 e-11	-2.679 e-13
F_{2x+y} (5 forces)	1	-	-	-	10	17.321	-5	-8.66	-0.067
	1000	-	-	-	10	17.321	-5	-8.66	-0.067
	∞	-	-	-	10	17.321	-5	-8.66	0.067
F_2 (4 forces)	1	-	-	-	2.834	-0.72	2.166	9.38	0.235
	1000	-	-	-	2.878	-0.53	2.122	9.19	-0.23
	∞	-	-	-	5	8.661	0	0	0

The described procedure proposed to find the analytical solution assuming the forces only in compression can be generalized. Moreover, the solution can be used for different loading. Analytical solutions for remaining types of simple monotonic loading will be solved in the same approach (simple tension and simple rotation of the dovetail joint). Those solutions will be later debugged on the basis of data obtained during experiments. The final objective is to propose an analytical solution of a dovetail joint possible to use for any case of loading.

Proposed solution is convenient for structural engineers, to assist the design of new joint or to verify the impact of interventions on existing timber structures.

ACKNOWLEDGMENT

Results presented in this paper are established on the basis of financial support of Ministry of Culture of the Czech Republic project NAKI – DF12P01OVV004 – Design and Assessment of Timber Joints of Historical Structures. Moreover the financial support of experimental campaign by STSM COST project FP1101 (COST-STSM-FP1101-16790) and assistance of the Laboratory of Structures of the University of Minho are gratefully acknowledged.

REFERENCES

Arciszewska-Kędzior, A., Kunecký, J., Hasníková, H. & Sebera, V. 2015. Lapped scarf joint with inclined faces and wooden dowels: Experimental and numerical analysis. *Engineering Structures*, *94(0)*: 1-8.

ASTM. 2014. *ASTM D143-14, Standard Test Methods for Small Clear Specimens of Timber*. West Conshohocken, PA: ASTM International.

Branco, J., Cruz, P., Piazza, M. & Varum, H. 2006a. Experimental analysis of original and strengthened traditional timber connections. *Proceedings of the 9th World Conference on Timber Engineering 2006, WCTE 2006*, Portland, OR, 1314-1321.

Branco, J., Cruz, P., Piazza, M. & Varum, H. 2006b. Modelling of timber joints in traditional structures. *Proceedings of the International Workshop on Earthquake Engineering on Timber Structures*, Coimbra, Portugal, 1 - 15.

CEN. 2003. *European Standard EN 338 2003 - Structural timber - Strength classes*. European committee for standardization.

CEN. 2006. *Standard in the Czech version of the European Standard EN 1995-1-1 2004 Eurocode 5 Design of timber structures including its Corrigendum EN 1995-1-1 2004/AC 2006-06*. European committee for standardization.

CEN. 2010. *European Standard EN 408 2010 - Timber structures – Structural timber and glued laminated timber – Determination of some physical and mechanical properties*. European committee for standardization.

Fajman, P. 2014. A scarf joint for reconstructions of historical structures. *2nd International Conference on Structural and Physical Aspects of Civil Engineering, SPACE 2013*.

Fajman, P. & Máca, J. 2014. The Effect of Key Stiffness on Forces in a Scarf Joint. In *Proceedings of the Ninth International Conference on Engineering Computational Technology*.

Jasienko, J., Engel, L. J. & Rapp, P. 2006. Study of strains and stresses in historical carpentry joints. In *Proceedings of the Structural Analysis of Historical Constructions*, New Delhi, 375-384.

Kunecký, J., Sebera, V., Hasníková, H., Arciszewska-Kędzior, A., et al. 2015. Experimental assessment of a full-scale lap scarf timber joint accompanied by a finite element analysis and digital image correlation. *Construction and Building Materials*, *76(0)*: 24-33.

Leijten, A. J. M., Jorissen, A. J. M. & de Leijer, B. J. C. 2012. The local bearing capacity perpendicular to grain of structural timber elements. *Construction and Building Materials*, *27(1)*: 54-59.

Leijten, A. J. M., Larsen, H. J. & Van der Put, T. A. C. M. 2010. Structural design for compression strength perpendicular to the grain of timber beams. *Construction and Building Materials*, *24(3)*: 252-257.

Parisi, M. A. & Cordié, C. 2010. Mechanical behavior of double-step timber joints. *Construction and Building Materials*, *24(8)*: 1364-1371.

Parisi, M. A. & Piazza, M. 2000. Mechanics of Plain and Retrofitted Traditional Timber Connections. *Journal of Structural Engineering*, *126(12)*: 1395.

Put, T. A. C. M. 2008. Derivation of the bearing strength perpendicular to the grain of locally loaded timber blocks. *Holz als Roh- und Werkstoff*, *66(6)*: 409-417.

Sangree, R. H. & Schafer, B. W. 2009a. Experimental and numerical analysis of a halved and tabled traditional timber scarf joint. *Construction and Building Materials*, *23(2)*: 615-624.

Sangree, R. H. & Schafer, B. W. 2009b. Experimental and numerical analysis of a stop-splayed traditional timber scarf joint with key. *Construction and Building Materials*, *23(1)*: 376-385.

Šobra, K., Branco, J. M. & Fajman, P. 2015. Behaviour of a dovetail joint solved using force analyses. In *Proceedings of the 3rd International Conference on Structural Health Assessment of Timber Structures*, Wroclaw, Poland (submitted for publication).

Villar, J. R., Guaita, M., Vidal, P. & Arriaga, F. 2007. Analysis of the Stress State at the Cogging Joint in Timber Structures. *Biosystems Engineering*, *96(1)*: 79-90.